CMS Physics Analysis Summary

Contact: cms-pag-conveners-heavyions@cern.ch 2012/08/13

Study of Z boson production with 150 μb^{-1} integrated PbPb luminosity at $\sqrt{s_{\mathrm{NN}}} = 2.76$ TeV

The CMS Collaboration

Abstract

This document presents the measurement of Z bosons in the di-muon channel in Pb-Pb collisions at $\sqrt{s_{NN}} = 2.76$ TeV made by the CMS experiment at the LHC. The analysis is based on a data sample collected during the PbPb run in 2011, which corresponds to an integrated luminosity of 150 μb^{-1}. The Z boson yield is investigated as a function of its rapidity and transverse momentum, as well as collision centrality. The results are compared to and agree with next-to-leading order theoretical predictions, scaled by the number of binary collisions.

1 Introduction

The W and Z bosons were first observed by the UA1 and UA2 experiments at CERN nearly thirty years ago in proton-antiproton collisions at $\sqrt{s}$ = 540 GeV [1, 2]. Since then, their properties have been characterised in detail by a succession of collider experiments. Their properties, such as their mass and their width (as well as their inclusive and differential cross sections) have been well measured at different centre-of-mass energies in electron-positron, proton-proton and proton-antiproton collisions. Thanks to its large centre-of-mass energy and delivered luminosities, the LHC offers the new opportunity to study W and Z boson production in nucleus-nucleus collisions. Based on the first lead-lead collisions corresponding to 7.2 μb^{-1} integrated luminosity, the CMS collaboration has reported first results on the $Z \to \mu\mu$ [3] and $W \to \mu\nu$ [4] processes, showing that electroweak bosons are essentially unmodified by the hot and dense medium created in heavy-ion collisions, often referred to as the quark-gluon plasma.

Once produced, electroweak bosons decay within the medium with a typical lifetime of 0.1 fm/c. Leptonic decays are thus of particular interest since leptons pass freely through the medium being probed, regardless of its nature (be it partonic or hadronic) or its properties. At first order, dileptons from Z bosons can thus serve as a reference to the processes expected to be heavily modified in the QGP, such as quarkonium production, or the production of an opposite-side jet in Z+jet processes [5]. However, in heavy-ion collisions, Z boson production can be slightly affected by initial-state effects. This modification is expected to be about 3% due to isospin effects [6], energy loss and multiple scattering of the initial partons [7]. In addition, parton distribution functions can be depleted (due to shadowing) and could modify the Z boson yield by at most 20% [6].

In this analysis, the study of Z production is reported with the second set of PbPb collisions that occurred in late 2011 and accounts for 150 μb^{-1} integrated luminosity. This 20-fold increase in statistics allows more detailed study of the transverse momentum (p_{T}), rapidity (y) and collision centrality dependencies of the Z boson yields.

2 The CMS detector

A detailed description of the CMS detector can be found in [8]. It is a general purpose apparatus with a silicon tracker detector, a lead tungstate crystal electromagnetic calorimeter (ECAL) and a brass scintillator hadron calorimeter (HCAL), all enclosed in a 3.8 T solenoidal magnetic field. The magnet is surrounded by an instrumented iron return yoke which encompasses gaseous detectors made of three technologies: Drift Tubes (DT), Cathode Strip Chambers (CSC), and Resistive Plate Chambers (RPC). In addition, CMS has hadron forward (HF) calorimeters which cover the pseudo–rapidity range $2.9 < |\eta| < 5.2$ and are used for triggering on minimum-bias PbPb collisions and defining collision centrality.

3 Event selection and trigger

In order to select a sample of pure inelastic hadronic collisions for analysis, the contamination from ultra-peripheral collisions and non-collision beam background are removed, as first explained in [9]. Events are preselected if they contain a reconstructed primary vertex made of at least two tracks, and an offline HF coincidence of at least three towers on each side of the interaction point with 3 GeV energy deposited in each tower. To further suppress the beam-gas and beam-scraping events, the length of pixel clusters along the beam direction is required to be compatible with particles originating from the event vertex.

These criteria select $(97 \pm 3)\%$ of hadronic collisions, corresponding to a number of minimum bias events $N_{MB} = 1.161$ billion for the sample analysed here. Assuming a PbPb cross-section of 7.65 barns, this translates into an integrated luminosity of 150 μb^{-1}. Only a fraction of these N_{MB} events is recorded by CMS, which uses a two-level trigger system to only select those events that are of particular interest. For the Z study presented here a trigger requiring two muons with p_T above 3 GeV/c is used.

The centrality of heavy-ion collisions, i.e. the geometrical overlap of the incoming nuclei, is related to the energy released in the collisions. In CMS, centrality is defined as percentiles of the distribution of the energy deposited in the HFs. The centrality classes used in this analysis are 50–100%, 40–50%, 40–30%, 30–20%, 20–10% and 0–10% (most central), ordered from the lowest to the highest HF energy deposit.

4 Muon reconstruction

The muon offline reconstruction algorithm starts by reconstructing tracks in the muon detectors, called stand-alone muons. These tracks are then matched to tracks reconstructed in the silicon tracker by means of an algorithm optimised for the heavy-ion environment [10, 11]. For muons from Z decays the tracking efficiency is $\simeq 85\%$, which is less than in the pp case. This is due to the fact that the track reconstruction in the heavy-ion environment requires more pixel hits to lower the number of combinations, due to the high multiplicity. Global fits of the muon and tracker tracks, called global muons, are used to obtain the results presented here. Background muons from cosmic rays and heavy-quark semileptonic decays are rejected by requiring a transverse (longitudinal) impact parameter of less than 0.3 (1.5) mm from the measured vertex. Other muon selection criteria are applied and are identical to the lower-luminosity publication [3].

5 Signal extraction

Figure 1 shows the dimuon invariant mass spectrum after the above mentioned criteria have been applied, and for opposite-charge muons (red full circles) in the 60–120 GeV/c^2 mass range. The individual muon pseudo–rapidity is required to be less than 2.4 and their p_T above 20 GeV/c, to ensure low background and high reconstruction efficiency. The dimuon rapidity is limited to $|y| < 2$. In the 60–120 GeV/c^2 mass range, 616 events are found with opposite-charge muons, and none with same-charge muons. The uncorrelated combinatorial background is thus much lower than 1%. The curve is a fit of the data to a Voigtian function representing the signal.

6 Acceptance and efficiency

In order to correct for the acceptance and efficiency, the electroweak process $Z \to \mu^+\mu^-$ has been simulated using the PYTHIA 6.424 [12] generator with isospin effects taken into account. The detector response to each PYTHIA signal event is simulated with GEANT4 [13] and then embedded in a realistic heavy-ion background event. These background events are produced with the HYDJET event generator [14] and then simulated with GEANT4 as well. The HYDJET parameters were tuned to reproduce the particle multiplicity for different centralities. The embedding is done at the level of detector hits and the signal and background event share the same generated vertex location. The embedded event is then processed through the trigger emulation and the full event reconstruction chain. Finally, the generated Z transverse momentum

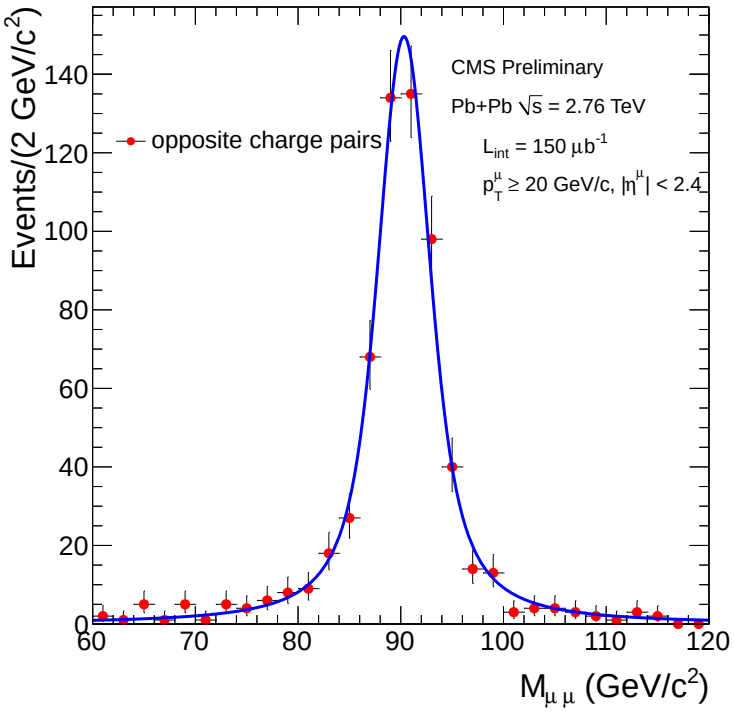

Figure 1: Dimuon invariant mass spectra. Full red circles are opposite-charge muon pairs, no same-charge muon pairs are observed in this range.

and the longitudinal vertex position are reweighted to match the one observed in data.

Though computed in one step, the acceptance (α) and efficiency (ε) correction can be split in two contributions as follow:

$$\alpha \times \varepsilon = \frac{N_{gen}(|y_Z| < 2.0, |\eta^\mu| < 2.4, p_T^\mu \geq 20)}{N_{gen}(|y_Z| < 2.0)} \times \frac{N_{rec}(|y_Z| < 2.0, |\eta^\mu| < 2.4, p_T^\mu \geq 20)}{N_{gen}(|y_Z| < 2.0, |\eta^\mu| < 2.4, p_T^\mu \geq 20)}$$

where N_{gen} is the number of generated Z applying the kinematical selection on the Z generated quantities and N_{rec} is the number of reconstructed dimuon applying the kinematical selection on the dimuon reconstructed quantities. It therefore corrects for resolution effects and final state radiation. When the data is binned in rapidity or p_T, the corresponding selection is applied on both the numerator and denominator. When integrated over p_T and rapidity, the acceptance and efficiency are approximately 70% and 60%, respectively. The centrality dependence of the efficiency is of the order of 10%.

7 Systematic uncertainties

The total systematic uncertainty on the Z yield is estimated by summing in quadrature different contributions. The most significant uncertainty is from the efficiency correction, and is calculated by comparing the agreement between simulation and data. The degree of agreement between simulation and data is estimated via the *tag-and-probe* technique in a similar way as in [15]. Three single-muon efficiencies are estimated (trigger, inner tracking and stand-alone muon identification) in both data and simulation and their degree of agreement are summed in quadrature and doubled to derive the uncertainty on dimuons. This results in an uncertainty of 8.7%. The uncertainty coming from the acceptance corrections are less than 2%, as estimated

by applying to the generated Z p_{T} and y distributions a weight that varies linearly from 0.7 to 1.3 (or from 1.3 to 0.7) over the ranges $0 < p_{\mathrm{T}} < 100$ GeV/c and $0 < |y| < 2.0$. The systematic uncertainty due to remaining background is estimated by fitting and extrapolating the lower di-muon mass range. Since a large part of the dimuon mass spectrum is composed of virtual photons, the virtual photon contribution is not subtracted and a conservative systematic uncertainty of 3% from remaining background is used as a systematic uncertainty on the yield.

8 Results

The yield of Z bosons (dN_{PbPb}/dy) is measured in PbPb collisions as a function of event centrality, and Z rapidity and p_{T}, and then compared to the pp cross section provided by a next-to-leading-order generator, scaled by the proper NN collision factor ($d\sigma_{pp}/dy \times T_{\mathrm{AA}}$, as described below and discussed in [16]).

The data is divided in different independent ranges: 6 in event centrality, 8 in rapidity, and 7 in p_{T}. the results are presented in figures 2, 3, and 4, respectively. The yields of $Z \to \mu^+\mu^-$ per minimum bias event and per unit of rapidity (and p_{T}) is computed as:

$$\frac{dN}{dy} = \frac{N(Z \to \mu^+\mu^-)}{\alpha\varepsilon N_{MB}\Delta y} \qquad \text{or} \qquad \frac{d^2N}{dydp_{\mathrm{T}}} = \frac{N(Z \to \mu^+\mu^-)}{\alpha\varepsilon N_{MB}\Delta y\Delta p_{\mathrm{T}}} \tag{1}$$

where $N(Z \to \mu^+\mu^-)$ is the number of counts found in the di-muon invariant mass range of 60–120 GeV/c^2, N_{MB} is the number of corresponding minimum bias events corrected for trigger efficiency (namely 1.161 billion events), α and ε are acceptance and efficiency corrections, and Δy and Δp_{T} are the bin range in consideration. When the Z yield is sliced according to centrality, N_{MB} is divided by the centrality fraction in consideration.

Figure 2 shows the centrality dependence of Z boson production in heavy-ion collisions. The obtained dN/dy yields per event are divided by the nuclear overlap function T_{AA}. This quantity is proportional to the number of elementary nucleon-nucleon binary collisions $N_{\mathrm{coll}} = T_{\mathrm{AA}} \times \sigma_{NN}$ where the latter is an assumed elementary NN cross section that cancels to first order in T_{AA}. At a given centrality, T_{AA} can be interpreted as the NN-equivalent integrated luminosity per AA collision, and T_{AA}-normalized yields can thus be directly compared to pp cross sections. In units of mb^{-1}, the average T_{AA} goes from 0.47 ± 0.07 to 23.2 ± 1.0, from the peripheral 50–100% to the central 0–10% centrality ranges. These numbers, as well as all centrality-related quantities summarized in table 1, are computed with a Glauber model [16]. It assumes the same parameters as in [17], namely standard parameters for the Woods-Saxon function that distributes the nucleons in the Pb nuclei, and a nucleon-nucleon inelastic cross section of $\sigma_{NN} = (64.5 \pm 5.0)$ mb, based on a fit of the existing data for total and elastic cross-sections in proton-proton and proton-antiproton collisions [18]. The T_{AA} uncertainties are derived by varying within uncertainties the Glauber parameters and the MB trigger and selection efficiency. They are included in the systematic uncertainties in figure 2. On the horizontal axis, the event centrality is translated in the average number of participants (N_{part}), through the same Glauber model.

No strong dependence of the $dN_{PbPb}/dy \times 1/T_{\mathrm{AA}}$ quantity is observed. The centrality-integrated value is displayed as an empty blue square and amounts to $dN_{PbPb}/dy \times 1/T_{\mathrm{AA}} = (56.9 \pm 2.0(\mathrm{stat.}) \pm 6.7(\mathrm{syst.}))$ pb. For comparison, the black line shows the cross-section of the $pp \to Z \to \mu^+\mu^-$ process provided by the POWHEG generator [19] interfaced with the PYTHIA

Table 1: The average numbers of participating nucleons N_{part}, average number of binary nucleon-nucleon collisions N_{coll}, and the average nuclear overlap function T_{AA} corresponding to the centrality ranges used in this analysis.

Centrality	N_{part}	N_{coll}	T_{AA} (mb^{-1})
$[50,100]\%$	22 ± 2	30 ± 5	0.47 ± 0.07
$[40,50]\%$	86 ± 4	176 ± 21	2.75 ± 0.30
$[30,40]\%$	130 ± 5	326 ± 34	5.09 ± 0.43
$[20,30]\%$	187 ± 4	563 ± 53	8.80 ± 0.58
$[10,20]\%$	261 ± 4	927 ± 81	14.5 ± 0.8
$[0,10]\%$	355 ± 3	1484 ± 120	23.2 ± 1.0
$[0,100]\%$	113.1 ± 2.9	363 ± 32	5.67 ± 0.32

parton-shower generator using CTEQ66 parton distribution functions [20]. Higher order corrections to this next-to-leading-order generator amount to 3% [21]. Typical next-to-next-to-leading-order calculations suffer themselves from another 3% uncertainty and are found to agree with high-precision 7 TeV pp data, as reported for instance in [22]. Therefore, a typical uncertainty of 5% is to be considered on this POWHEG reference curve, which thus amounts to $d\sigma_{pp}/dy(|y| < 2.0) = (59.6 \pm 3.0)$ pb. It is found to agree with the PbPb yields divided by T_{AA}. This shows that the Z production scales with the number of binary NN collisions and that nuclear effects such as isospin or shadowing are small compared to the experimental uncertainties.

The distributions dN/dy as a function of rapidity and $d^2N/dydp_{\text{T}}$ as a function of p_{T} are also compared to POWHEG on figures 3 and 4. Since data is here integrated over centrality, the POWHEG reference is multiplied by the minimum bias $T_{\text{AA}} = (5.67 \pm 0.32)$ mb^{-1} as provided by the Glauber model described above[1]. No strong deviations from this absolutely-normalized reference are observed.

Table 2 summarizes all the observed yields.

9 Conclusions

The Z-boson yields in PbPb collisions at $\sqrt{s_{\text{NN}}} = 2.76$ TeV have been measured as a function of transverse momentum, rapidity and event centrality in the dimuon channel with about 150 μb^{-1} integrated luminosity. Within uncertainties, no centrality dependence is observed once the yields are normalized to the number of elementary collisions. Neither rapidity nor transverse momentum modifications are observed with respect to theoretical next-to-leading order pQCD nucleon-nucleon cross sections scaled by the number of elementary collisions. The total Z yield per event and per unit of rapidity, divided by the pp-equivalent luminosity, $dN_{PbPb}/dy \times 1/T_{\text{AA}} = (56.5 \pm 2.0(\text{stat.}) \pm 7.1(\text{syst.}))$ pb, is found to agree with corresponding next-to-leading order pp cross-section $d\sigma_{pp}/dy = (59.6 \pm 3.0)$ pb. The Z production is thus proportional to the number of binary NN collisions and nuclear effects such as isospin or shadowing are small compared to the experimental uncertainties.

[1]By construction, this minimum bias T_{AA} is equal to A^2/σ_{PbPb}, where $A = 208$ is the lead atomic number and $\sigma_{PbPb} = (7.65 \pm 0.42)$ barns is the total PbPb inelastic cross section computed from the same Glauber model.

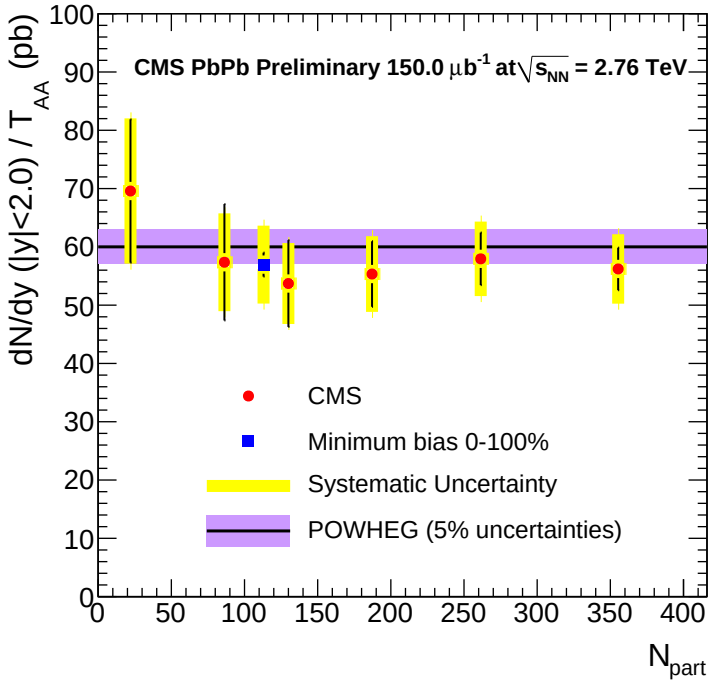

Figure 2: Event centrality dependence of the $Z \to \mu\,\mu$ yield per event divided by the expected average nuclear overlap function T_{AA}. The vertical scale equivalently corresponds to Z yields per binary collision (N_{coll}) times the nucleon-nucleon cross section, and is thus directly comparable to the pp cross section from the POWHEG generator displayed as a black line. On the horizontal axis, event centrality is depicted as the average number of participating nucleons N_{part} from 22 to 355, spanning an average N_{coll} of 30 to 1484. Vertical lines (bands) correspond to statistical (systematic) uncertainties.

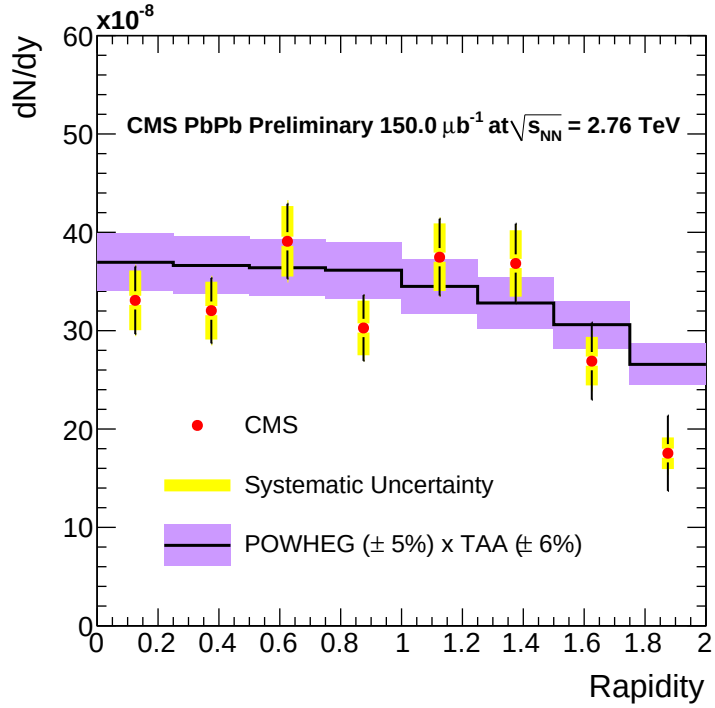

Figure 3: $Z \rightarrow \mu\ \mu$ yields versus the Z boson rapidity. Theoretical predictions are described in the text. The black solid line comes from the POWHEG pp generator, multiplied by T_{AA}.

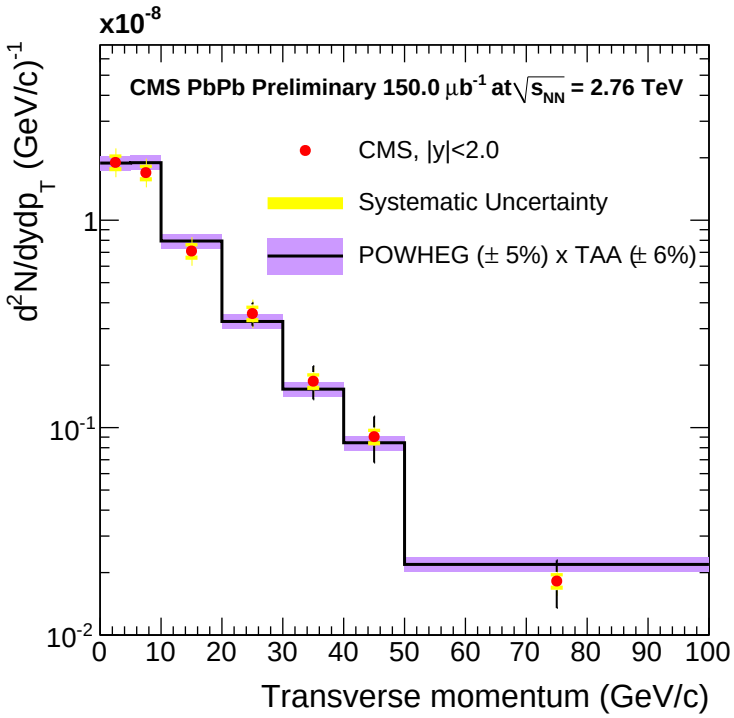

Figure 4: $Z \rightarrow \mu\ \mu$ yields versus the Z boson transverse momentum. Vertical lines (bands) correspond to statistical (systematic) uncertainties. The black solid line comes from the POWHEG pp generator, scaled by T_{AA}.

Table 2: For each $|y|$, p_{T} and centrality interval, number of Z bosons N_{Z}, associated yield per event dN/dy, $d^2N/dydp_{\mathrm{T}}$ in units of $(GeV/c)^{-1}$, and dN/dy $\times 1/\mathrm{T_{AA}}$ in units of pb. The first uncertainty is statistical and the second systematic.

$\lvert y\rvert$	N_{Z}	dN/dy (10^{-8})
$[0, 0.25]$	93	$33.1 \pm 3.4 \pm 3.0$
$[0.25, 0.5]$	93	$32.0 \pm 3.3 \pm 2.9$
$[0.5, 0.75]$	105	$39.1 \pm 3.8 \pm 3.6$
$[0.75, 1.0]$	82	$30.3 \pm 3.3 \pm 2.7$
$[1.0, 1.25]$	92	$37.5 \pm 3.9 \pm 3.4$
$[1.25, 1.5]$	83	$36.8 \pm 4.0 \pm 3.4$
$[1.5, 1.75]$	47	$26.9 \pm 3.9 \pm 2.5$
$[1.75, 2.0]$	21	$17.5 \pm 3.8 \pm 1.6$
$p_{\mathrm{T}}(GeV/\mathrm{c})$	N_{Z}	$d^2N/dydp_{\mathrm{T}}$ $(10^{-8}$ $(\mathrm{GeV}/c)^{-1})$
$[0, 5]$	192	$1.89 \pm 0.14 \pm 0.18$
$[5, 10]$	167	$1.70 \pm 0.13 \pm 0.16$
$[10, 20]$	131	$0.71 \pm 0.06 \pm 0.06$
$[20, 30]$	63	$0.35 \pm 0.04 \pm 0.03$
$[30, 40]$	30	$0.17 \pm 0.03 \pm 0.01$
$[40, 50]$	16	$0.09 \pm 0.02 \pm 0.01$
$[50, 100]$	15	$0.018 \pm 0.005 \pm 0.002$
Centrality	N_{Z}	$dN/dy(\lvert y\rvert < 2.0)/T_{\mathrm{AA}}$ (pb)
$[50, 100]\%$	237	$56.2 \pm 3.6 \pm 5.9$
$[40, 50]\%$	165	$57.9 \pm 4.5 \pm 6.4$
$[30, 40]\%$	97	$55.3 \pm 5.6 \pm 6.5$
$[20, 30]\%$	52	$53.7 \pm 7.4 \pm 6.9$
$[10, 20]\%$	33	$57.3 \pm 10.0 \pm 8.4$
$[0, 10]\%$	32	$69.6 \pm 12.3 \pm 12.5$
$[0, 100]\%$	616	$56.9 \pm 2.0 \pm 6.7$

Acknowledgments

We congratulate our colleagues in the CERN accelerator departments for the excellent performance of the LHC machine. We thank the technical and administrative staff at CERN and other CMS institutes, and acknowledge support from: BMWF and FWF (Austria); FNRS and FWO (Belgium); CNPq, CAPES, FAPERJ, and FAPESP (Brazil); MES (Bulgaria); CERN; CAS, MoST, and NSFC (China); COLCIENCIAS (Colombia); MSES (Croatia); RPF (Cyprus); MoER, SF0690030s09 and ERDF (Estonia); Academy of Finland, MEC, and HIP (Finland); CEA and CNRS/IN2P3 (France); BMBF, DFG, and HGF (Germany); GSRT (Greece); OTKA and NKTH (Hungary); DAE and DST (India); IPM (Iran); SFI (Ireland); INFN (Italy); NRF and WCU (Korea); LAS (Lithuania); CINVESTAV, CONACYT, SEP, and UASLP-FAI (Mexico); MSI (New Zealand); PAEC (Pakistan); MSHE and NSC (Poland); FCT (Portugal); JINR (Armenia, Belarus, Georgia, Ukraine, Uzbekistan); MON, RosAtom, RAS and RFBR (Russia); MSTD (Serbia); SEIDI and CPAN (Spain); Swiss Funding Agencies (Switzerland); NSC (Taipei); TUBITAK and TAEK (Turkey); STFC (United Kingdom); DOE and NSF (USA). Individuals have received support from the Marie-Curie programme and the European Research Council (European Union); the Leventis Foundation; the A. P. Sloan Foundation; the Alexander von Humboldt Foundation; the Austrian Science Fund (FWF); the Belgian Federal Science Policy Office; the Fonds pour la Formation à la Recherche dans l'Industrie et dans l'Agriculture (FRIA-Belgium); the Agentschap voor Innovatie door Wetenschap en Technologie (IWT-Belgium); the Council of Science and Industrial Research, India; the Compagnia di San Paolo (Torino); and the HOMING PLUS programme of Foundation for Polish Science, cofinanced from European Union, Regional Development Fund.

References

[1] UA1 Collaboration Collaboration, "Experimental Observation of Lepton Pairs of Invariant Mass Around 95-GeV/c**2 at the CERN SPS Collider", *Phys.Lett.* **B126** (1983) 398–410, doi:10.1016/0370-2693(83)90188-0.

[2] UA2 Collaboration Collaboration, "Evidence for $Z^0 \to e^+e^-$ at the CERN $\bar{p}p$ Collider", *Phys.Lett.* **B129** (1983) 130–140, doi:10.1016/0370-2693(83)90744-X.

[3] CMS Collaboration, "Study of Z boson production in PbPb collisions at nucleon-nucleon centre of mass energy = 2.76 TeV", *Phys.Rev.Lett.* **106** (2011) 212301, arXiv:1102.5435.

[4] CMS Collaboration, "Study of W boson production in PbPb and pp collisions at sqrt(s[NN]) = 2.76 TeV", arXiv:1205.6334.

[5] R. V.Kartvelishvili and R.Shanidze, "On Z and Z+jet production in heavy ion collisions", *Phys.Lett.B* **356** (1995) 589.

[6] H.Paukkunen and C.A.Salgado, "Constraints for the nuclear parton distributions from Z and W production at the LHC", *JHEP* **1103** (2011) 071.

[7] I. R.B.Neufeld and B.W.Zhang, "Toward a determination of the shortest radiation length in nature", arXiv:1010.3708.

[8] CMS Collaboration, "The CMS experiment at the CERN LHC", *Phys.Rev.C* (2011).

[9] CMS Collaboration, "Observation and studies of jet quenching in PbPb collisions at nucleon-nucleon center-of-mass energy = 2.76 TeV", *JINST* (2008).

[10] CMS Collaboration, "Track reconstruction in heavy ion events using the CMS tracker", *Nucl. Instrum. Meth.* **A566** (2006) 123, doi:10.1016/j.nima.2006.05.023.

[11] CMS Collaboration, "CMS physics technical design report: Addendum on high density QCD with heavy ions", *J. Phys.* **G34** (2007) 2307, doi:10.1088/0954-3899/34/11/008.

[12] T. Sjöstrand, S. Mrenna, and P. Skands, "PYTHIA 6.4 physics and manual", *JHEP* **05** (2006) 026, arXiv:hep-ph/0603175.

[13] GEANT4 Collaboration, "GEANT4: A simulation toolkit", *Nucl. Instrum. Meth.* **A506** (2003) 250, doi:10.1016/S0168-9002(03)01368-8.

[14] I. P. Lokhtin and A. M. Snigirev, "A model of jet quenching in ultrarelativistic heavy ion collisions and high-p(T) hadron spectra at RHIC", *Eur. Phys. J.* **C45** (2006) 211, doi:10.1140/epjc/s2005-02426-3, arXiv:hep-ph/0506189.

[15] CMS Collaboration, "Suppression of non-prompt J/psi, prompt J/psi, and Y(1S) in PbPb collisions at sqrt(sNN) = 2.76 TeV", *JHEP* **1205** (2012) 063, arXiv:1201.5069.

[16] M. L. Miller et al., "Glauber modeling in high energy nuclear collisions", *Ann. Rev. Nucl. Part. Sci.* **57** (2007) 205, doi:10.1146/annurev.nucl.57.090506.123020, arXiv:nucl-ex/0701025.

[17] CMS Collaboration, "Observation and studies of jet quenching using dijet momentum imbalance in PbPb collisions at $\sqrt{s_{NN}} = 2.76$ TeV with the CMS detector", *submitted to Phys. Rev. C*, arXiv:1102.1957.

[18] Particle Data Group Collaboration, "Review of particle physics", *J. Phys.* **G37** (2010) 075021, doi:10.1088/0954-3899/37/7A/075021.

[19] S. Alioli, P. Nason, C. Oleari et al., "NLO vector-boson production matched with shower in POWHEG", *JHEP* **07** (2008) 060, doi:10.1088/1126-6708/2008/07/060, arXiv:0805.4802.

[20] J. Pumplin et al., "New generation of parton distributions with uncertainties from global QCD analysis", *JHEP* **07** (2002) 012, arXiv:hep-ph/0201195.

[21] S. Catani, L. Cieri, G. Ferrera et al., "Vector boson production at hadron colliders: A Fully exclusive QCD calculation at NNLO", *Phys.Rev.Lett.* **103** (2009) 082001, doi:10.1103/PhysRevLett.103.082001, arXiv:0903.2120.

[22] CMS Collaboration Collaboration, "Measurement of the Inclusive W and Z Production Cross Sections in pp Collisions at sqrt(s) = 7 TeV", *JHEP* **1110** (2011) 132, doi:10.1007/JHEP10(2011)132, arXiv:1107.4789.